

# Influence of Different Amides as Plasticizer on the Properties of Soy Protein Plastics

Dagang Liu, Huafeng Tian, Lina Zhang

Department of Chemistry, Wuhan University, Wuhan 430072, China

Received 11 September 2006; accepted 30 March 2007

DOI 10.1002/app.26656

Published online 15 June 2007 in Wiley InterScience (www.interscience.wiley.com).

**ABSTRACT:** A series of amide-plasticized soy protein isolate materials were prepared by hot compression-molding techniques at 140°C and 20 MPa. The plasticizing efficiency of amides was in the order of formamide > acetamide > acrylamide resulting from scanning electron microscopy, optical transmittance and differential scanning calorimetry. The results from torque rheology indicated that flowability and processability could be improved by adding amide as plasticizers. All of the sheets showed single glass transition temperature obtained by differential scanning calorimetry, indicating good compatibility between amide and soy protein. The water

uptake of the plastics sheets and effects of moisture content on the thermal and mechanical properties were also investigated. The glass transition temperature and tensile strength decreased with an increase of moisture content in sheets. Formamide was considered as the best plasticizer of three amides because of the higher plasticizing efficiency and water resistance of SFm sheets. © 2007 Wiley Periodicals, Inc. *J Appl Polym Sci* 106: 130–137, 2007

**Key words:** soy protein plastics; amide; plasticizing efficiency

## INTRODUCTION

Soy proteins, the co-products from the soybean oil industry, have been used as functional and nutritional ingredients in food. Currently, soy protein-based plastics,<sup>1–5</sup> adhesives,<sup>6–8</sup> films,<sup>9,10</sup> and coatings are being considered for applications such as agricultural equipment, marine infrastructure, and civil engineering.<sup>11–14</sup> Soy protein materials have been extensively researched as environment-friendly, fully biodegradable, and sustainable “green” alternatives. In exploring alternative raw materials to replace the traditional petroleum resources, soy protein has been considered to be a great potential because of their renewability, biodegradability, and relatively low cost.

For successful processing of soy protein isolate (SPI), a simple and effective way is to plasticize soy protein by polyols such as glycerol, propylene glycol, triethylene glycol, ethylene glycol, butane diols, or by water. The plasticized SPI powder can be thermally pressed or extruded into plastic sheets with less brittleness.<sup>15</sup> However, two inherent problems

have limited the uses of soy protein based plastics, namely high moisture sensitivity and relatively low mechanical properties. For example, water and glycerol plasticized soy protein materials increase the moisture sensitivity and greatly reduce the tensile strength and modulus.<sup>16–18</sup> Amide is a representative compound for peptide linkage in polypeptides and proteins since the amide bond makes up the backbones of peptides and protein.<sup>19</sup> In our previous paper, a novel plasticizer-acetamide has been successfully used as a plasticizer for SPI.<sup>20</sup> The results showed that the acetamide plasticized plastics had good thermal stability and water-resistance. Herein, other two amides, formamide and acrylamide, will be used as plasticizers for SPI to compare with acetamide in this work. So an attempt was made to investigate the plasticizing efficiency of the three plasticizers as well as properties of soy protein plastics. In addition, the effect of the moisture on the properties of SPI plastics was also discussed.

## EXPERIMENTAL

### Materials

Commercial SPI was purchased from Dupont-Yunmeng Protein Technology (Yunmeng, China). The weight-average molecular weight ( $M_w$ ) of SPI was determined by multi-angle laser light scattering instrument equipped with a He-Ne laser ( $\lambda = 632.8$  nm) (DAWN<sup>®</sup> DSP, Wyatt Technology, USA) and was found to be  $20.5 \times 10^4$  g/mol. The original

Correspondence to: L. Zhang (lnzhang@public.wh.hb.cn).

Contract grant sponsor: National Natural Science Foundation of China; contract grant numbers: 59933070, 20474048.

Contract grant sponsor: Key Laboratory of Cellulose Chemistry, Guangzhou Institute of Chemistry, Chinese Academy of Sciences.

moisture content, protein content, and amino acid compositions of SPI have been investigated in our laboratory.<sup>21</sup> Formamide ( $M_w = 45.04$  g/mol), acetamide ( $M_w = 59.07$  g/mol), and acrylamide ( $M_w = 71.08$  g/mol) were used as plasticizers, respectively. These plasticizers were of analytical-grade and were purchased from the Tianjin fiducial Chemical Co. (Tianjin, China). All the reagents were kept in desiccators with  $P_2O_5$  as desiccant during experiment period.

### Compression-molded sheets

The amount of plasticizer in the SPI material can be described in terms of the phr (part per hundred parts of resin) ratio, here which accounts for the percent mass ratio of the plasticizer to the SPI in grams, and was defined as:

$$\text{phr} = \frac{\text{mass of plasticizer}}{\text{mass of SPI}} \times 100 \quad (1)$$

SPI with desired formamide, acetamide, or acrylamide content (10–50 phr) was mixed in a mortar, and then was crushed up in a kitchen beater (HR1704, Philips, Zhuhai, China) for 15 min, respectively. Subsequently, the resultant mixture was placed in a mold covered with two polished stainless-steel plates and then was compression-molded with a hot press as described previously.<sup>21</sup> The sheets were molded at 140°C under the pressure of 20 MPa for 10 min, and then air-cooled to 40°C under the same pressure with the cooling rate of about 3°C/min before the removal from the mold. Three series of compression-molded sheets were coded as SFm, SAm, and SAc, corresponding to the formamide, acetamide, and acrylamide plasticized protein sheets, respectively. It was worth noting that when formamide content was more than 30 phr, the powder could not be processed into perfect plastic sheets because of high flowability. Thus formamide contents were from 10 to 30 phr, but both acetamide and acrylamide contents were from 10 to 50 phr. All of the resulting sheets were conditioned in vacuum at 60°C until constant weight, and then stored in dry condition to provide a 0% relative humidity (RH) with  $P_2O_5$  before analysis.

### Sample conditioning and water uptake

All the sheets were conditioned in desiccators with  $P_2O_5$  as desiccant (0% relative humidity) at room temperature to give an initial weight ( $W_0$ ). The moisture content of the amide-plasticized SPI sheets was achieved by conditioning the samples at room temperature in desiccators with  $CaCl_2 \cdot 6H_2O$ ,  $K_2CO_3 \cdot 2H_2O$ ,  $NaBr \cdot 2H_2O$ ,  $NaCl$ , and  $CuSO_4 \cdot 6H_2O$  saturated salt solutions to provide a relative humidity (RH) of 35, 43,

58, 75, and 98%, respectively.<sup>22–24</sup> The sheets with rectangular dimensions of 20 mm × 10 mm × 0.4 mm were weighed to obtain the weight  $W_t$ . The water content or water uptake (WU) of the sheets was calculated as following equation<sup>25</sup>:

$$\text{WU}(\%) = \frac{W_t - W_0}{W_0} \times 100 \quad (2)$$

### Characterization

Percent optical transmittance (Tr) of the sheets with a thickness of about 0.4 mm was measured with an ultraviolet-visible spectrometer (UV-160A, Shimadzu, Japan) in the wavelength range from 800 to 200 nm. Scanning electron microscopy (SEM) images were taken on an S-570 microscope (Hitachi, Japan). The dry sheets were frozen in liquid nitrogen and snapped immediately, and then the fractured faces of the sheets were coated with gold for SEM observations.

Haake rheomix test was used to measure the melt flow property of SFm, SAm, and SAc plastics. Each of the samples was crushed up into powders by the kitchen beater. Dry SPI and amide/SPI powder (about 5 g) were added into a Haake MiniLab (Micro Rheology Compounder, Germany) to obtain torque values at 160°C with the shear rate of 50 rpm. Differential scanning calorimetry (DSC) was carried out on a Diamond DSC apparatus (Perkin-Elmer, USA) equipped with a cooler system with liquid nitrogen. Dry sample (about 10 mg) was placed in pressure-tight aluminum DSC cells under nitrogen atmosphere from −150 to 200°C with the heating rate of 10°C/min. Glass transition temperature ( $T_g$ ) was taken as the mid-point of the specific heat increment at the glass-rubber transition. Thermogravimetric analysis (TGA) was carried out on a Pyris TGA linked to a Pyris diamond TA lab system (Perkin-Elmer) at a heating rate of 10°C/min between 25 and 500°C under nitrogen atmosphere. The mass of the samples for TGA test was approximately 5 mg.

Tensile strength ( $\sigma_b$ ), elongation at break ( $\varepsilon_b$ ), and Young's modulus ( $E$ ) of the sheets were measured on a universal testing machine (CMT6503, Shenzhen SANS Test Machine, Shenzhen, China) with a tensile rate of 5 mm/min according to ISO 527-3: 1995 (E). An average value of five replicates of each sample was taken.

## RESULTS AND DISCUSSION

### Plasticizing efficiency of amides

Figure 1 shows SEM micrographs of the fractured surface of the SFm20, SAm20, and SAc20 sheets conditioned at 0% RH. The SFm20 sheet exhibits

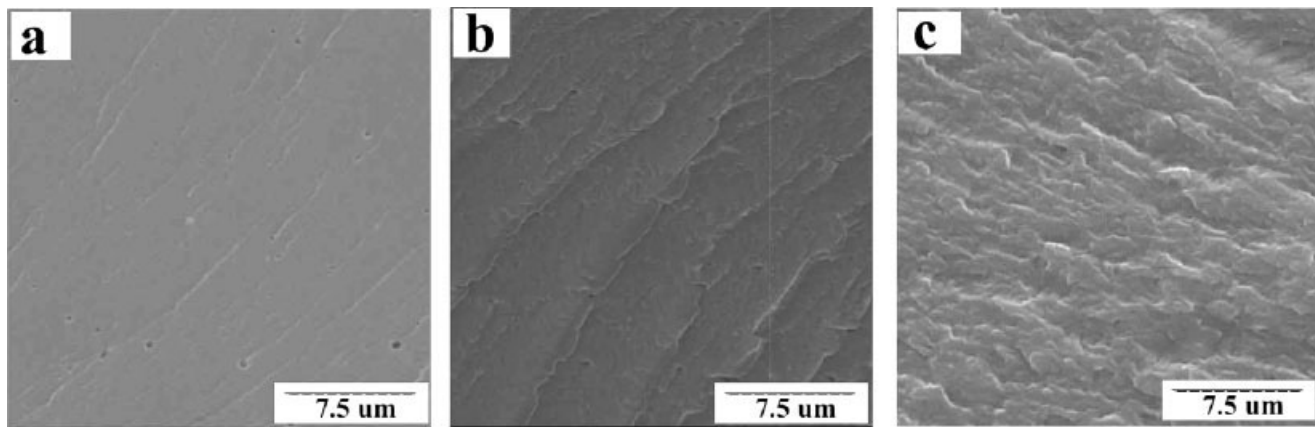


**Figure 1** SEM micrographs of the fractured surface of the SFm20 (a), SAM20 (b), and SAc20 (c) sheets conditioned at 0% RH.

smoother cross-section than the other two. Generally, the transparency of the materials is an auxiliary criterion to judge the compatibility of the composites.<sup>26</sup> Dependence of Tr on amide contents (from 10 to 30 phr) for the SFm, SAM, and SAc sheets at different wavenumber conditioned at 0% RH is shown in Figure 2. During the range of 200–400 nm the Tr values of the SFm, SAM, and SAc sheets are nearly 0 because aromatic amino acid of soy protein can absorb ultraviolet light. However, the sheets show high transmittance in the visible region and their Tr values increase with an increase of wave number from 400 to 800 nm. When the content of formamide is 20 phr, SFm20 sheet exhibit higher Tr values than other SFm sheets, which means the most homogeneous structure occurred in SFm sheets comparing to others, that is to say the best plasticizing effect was

obtained. Furthermore, the best plasticizing effects for SAM and SAc sheets were obtained when the content of acetamide and acrylamide was 30 phr, respectively. In addition, the Tr value of SFm20 is higher than SAM20 and SAc20, and even higher than SAM30 and SAc30.

Usually, glass transition temperature ( $T_g$ ) of plastics can reflect plasticizing effects of the plasticizer. DSC curves of pure SPI, SFm20, SAM20, and SAc20 conditioned at 0% relative humidity are shown in Figure 3 and obtained  $T_g$  values of the SFm, SAM, and SAc sheets from DSC are summarized in Table I. It has been reported that polyols such as glycerol-plasticized SPI plastics showed at least two  $T_g$ s assigned to glycerol-rich and protein-rich domains, respectively. It meant that obvious phase separation happened.<sup>17</sup> In this work pure soy protein shows no

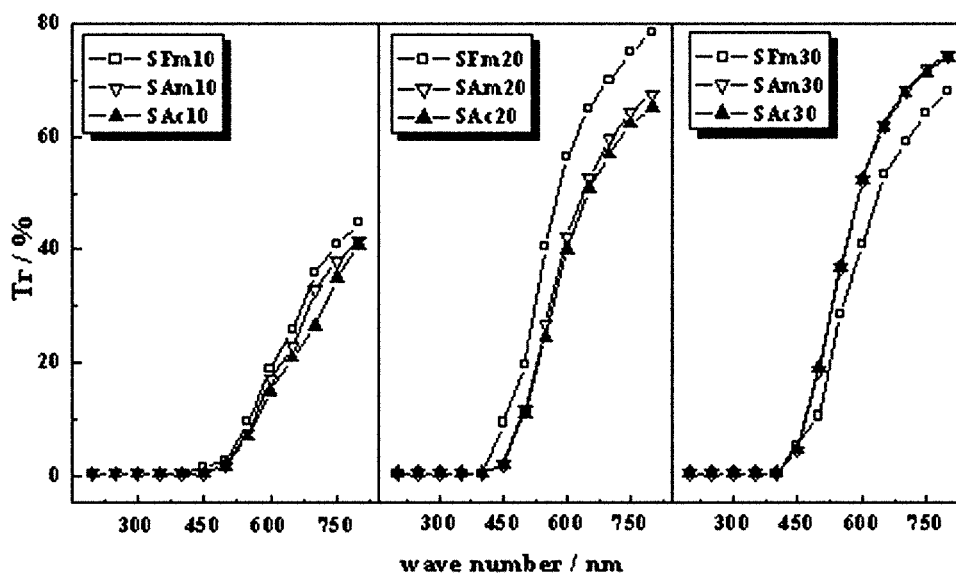


**Figure 2** Dependence of Tr on amide contents for the SFm, SAM, and SAc sheets at different wavenumber conditioned at 0% RH.

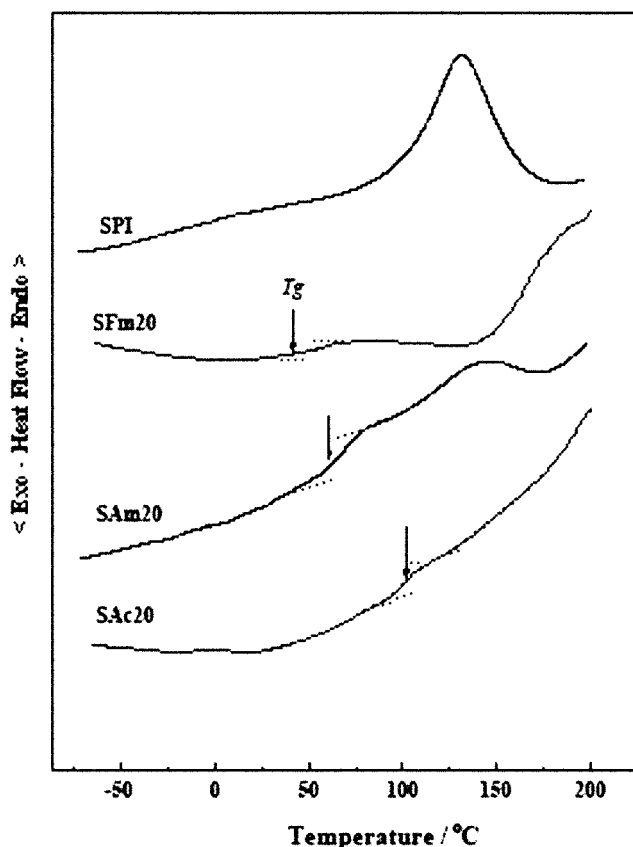


**Figure 3** DSC thermograms of SFm20, SAm20, SAc20, and pure SPI.

glass transition. However, soy protein materials plasticized by amides (SFm, SAm, and SAc) exhibit single glass transition and imply homogenous structure. This can be explained that the structure and polarity of three amides are similar to protein polypeptides resulting in a good compatibility between them. As shown in Table I with an increase of plasticizer contents, the  $T_g$  values decreases. Although good plasticizing effect is obtained, different effect stems from different plasticizer.  $T_g$ s of the sheets are in the order

of SAc20 > SAm20 > SFm20, and even  $T_g$  of SFm20 is lower than any other SAm and SAc sheets, indicating better plasticizing efficiency of formamide than other amides. Changes in heat capacity increment ( $\Delta C_p$ ) have usually been regarded as the characteristic thermodynamic signature of order-disorder transitions in homogeneous systems, particularly those comprising hydrogen-bonded networks.<sup>27</sup> As shown in Table I, the  $\Delta C_p$  of the materials increases with the plasticizer content, and SAc sheets exhibit higher  $\Delta C_p$  values than SFm and SAm sheets. As we know, strong intra- and intermolecular interactions in SPI caused by extensive hydrogen bonding limit the mobility of the protein molecular chain. However, amide plasticizers can penetrate into the protein chains and interact with soy protein by hydrogen bonding, which has been evidenced by the FTIR in early work.<sup>20</sup> It is not difficult to find that the hydrogen bond-forming abilities of three amides are different. At first, formamide has lower molecular weight and less steric hindrance than acetamide and acrylamide. Furthermore, the double bonding conjugate structure of acrylamide also weakened hydrogen bonding with protein. Therefore, the hydrogen bond-forming abilities of three amides are in the order of formamide > acetamide > acrylamide. Hydrogen-bonding interaction between formamide and SPI is stronger than others, and thus formamide easily penetrate into protein, screen strong interaction between protein chains, and make protein chains move more easily. Thus, the plasticizing efficiency of three amides are in order of formamide > acetamide > acrylamide.

#### Effects of amide on the properties of plasticized SPI

Torque rheometer can provide quantitative information on the melt flow behavior of the macromolecular materials. The pure SPI could not melt well at

**TABLE I**  
 $T_g$  and  $\Delta C_p$  Values of the SFm, SAm, and SAc Sheets Obtained from DSC at Different Relative Humidity

	0% RH		35% RH ( $T_{gi}$ : °C)	43% RH ( $T_{gi}$ : °C)	58% RH ( $T_{gi}$ : °C)	75% RH ( $T_{gi}$ : °C)	98% RH ( $T_{gi}$ : °C)
	$T_g$ (°C)	$\Delta C_p$ (J/g °C)					
SFm10	51.9	0.233					
SFm20	44.6	0.268	28.2	-10.5	-25.1	-47.2	-62.3
SAm10	80.2	0.354					
SAm20	77.5	0.445	32.1	-5.6	-20.7	-52.1	-69.8
SAm30	75.1	0.471					
SAm40	72.8	0.525					
SAm50	71.4	0.533					
SAc10	111.0	0.614					
SAc20	97.2	0.683	63.3	32.4	1.5	-24.7	-66.7
SAc30	90.2	0.848					
SAc40	79.6	0.909					
SAc50	76.7	0.917					

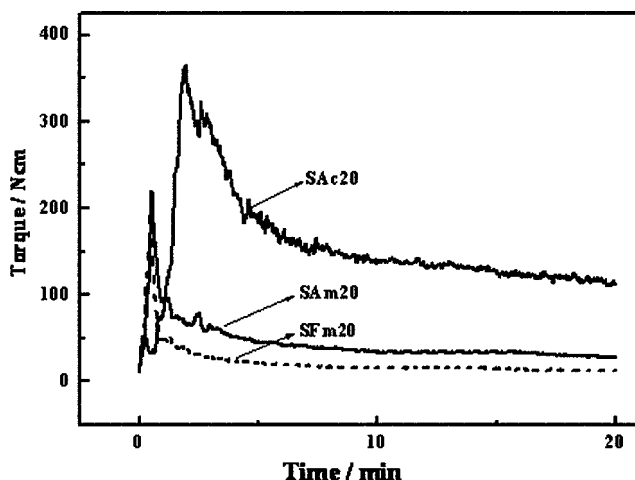


**Figure 4** Torque-time plots of SFm20, SAm20, and SAc20 at 50 rpm and 160°C.

160°C, but its melting behavior could be improved at 200°C. With addition of amides, the plasticized SPI samples were melted well at 160°C. Figure 4 shows torque against time plots of SFm20, SAm20, and SAc20 at 50 rpm and 160°C. With a progress of measurement, the torque increases rapidly to a maximum and then decreases to a stable value accompanying with the phenomena that the solid powder turned into melt fluid state. With an increase of the plasticizer content the torque decreases sharply. The torque development is associated with a change in consistency from a powder to a cohesive and elastic material.<sup>28,29</sup> Figure 5 shows the effect of amide plasticizer on maximum torque and equilibrium torque of SFm, SAm, and SAc. The maximum torque and equilibrium torque values are in the order of SFm < SAm < SAc at the same plasticizer content. The equilibrium torques of SFm, SAm, and SAc change slightly, indicating fully plasticization after the phr contents of formamide, acetamide, and acrylamide reach 20, 20, and 30,

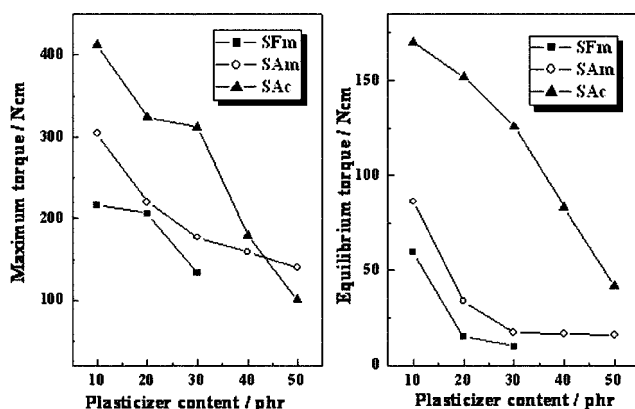


**Figure 5** Effect of amide contents on the maximum torque and equilibrium torque of SFm, SAm, and SAc.

respectively. Accordingly, the time to achieve the peak torque and the time to achieve the equilibrium torque for SFm20 are shorter than others as observed from Figure 4. On the basis of above results it can be concluded that formamide is more effective in reducing the processing temperature and improving the flexibility of soy protein.

TG and DTG curves of pure SPI, SFm, SAm, and SAc sheets conditioned at 0% RH are shown in Figure 6. SPI degrades by a two-step process whereas degradation of the amide-plasticized soy protein consists of three weight loss steps. The weight loss in the first stage (below 150°C) is assigned to the evaporation of residual moisture, and the second step from 150 to 250°C can be attributed to the evaporation of a part of plasticizer, and the final step is mainly due to the degradation of soy protein. With the increase of amide content the weight loss of the second step and the last step increases. The weight loss from 150 to 250°C of SFm20, SAm20, and SAc20 are 8, 10.6, and 11.9%, respectively. Although the boiling point of formamide is lower than acetamide and acrylamide, the evaporation of SFm20 is relatively low, indicating compact adhesion action between formamide and SPI. Amide-plasticized SPI materials have similar thermal degradation and have good thermal stability as observed by the mass fraction of residues.

Water uptake on solid-state protein is a result of the hydrophilic and ionized groups of the protein. The amount of water in the protein is determined by equilibration of samples at a given relative humidity and has a significant impact on the properties of protein.<sup>30</sup> Figure 7 shows the water uptake isotherm

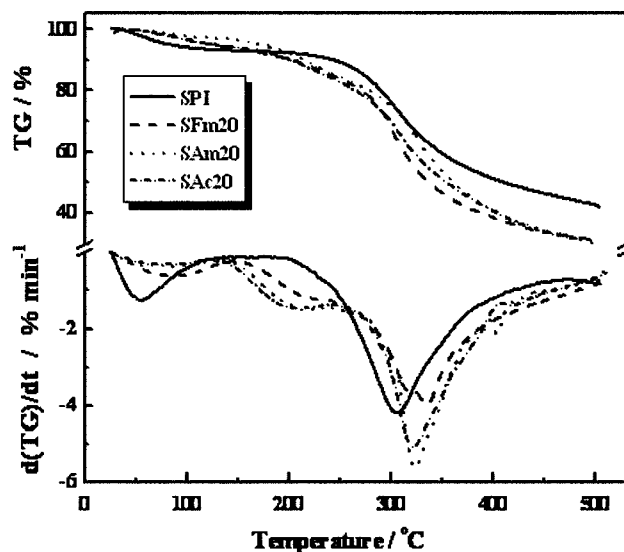


**Figure 6** TG and DTG thermograms of the SFm20, SAm20, and SAc20 sheets as well as pure SPI conditioned at 0% RH.

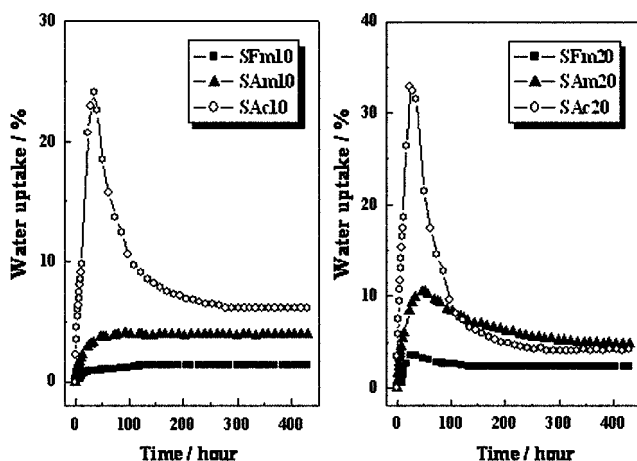


Figure 7 Water uptake isotherm of the SFm, SAM, and SAc sheets conditioned at 35% RH and ambient temperature.

of the SFm, SAM, and SAc sheets conditioned at 35% RH and ambient temperature. Water uptake isothermal curves are broadly similar in form to Type II isotherm described by Brunauer.<sup>31-33</sup> Water uptake of the sheets (except SFm10 and SAM10) exhibit two-stage water sorption profiles. In the first step, there is an increase in water uptake with time until maximum value and then decrease in values till equilibrium is reached. In fact the absorption of water was fast at short times ( $t < 100$  h), and then adsorptions took place at extended times. The maximum water uptake of the sheets increases with an increase of the plasticizer contents, and their values for SFm20, SAM20, and SAc20 sheets are 3.6, 10.5, and 32.8%, respectively.

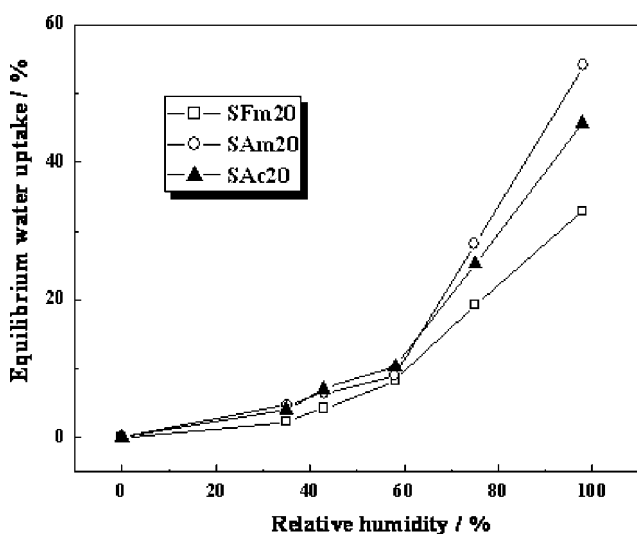


Figure 8 Effect of different RH levels on the equilibrium water uptake of SFm20, SAM20, and SAc20 sheets at ambient temperature.

Obviously, SFm20 exhibits a better water-resistance than SAM20 and SAc20 as a result of more compact structure of SFm20 sheet than others as shown in SEM micrographs.

**Effects of RH on properties of amide-plasticized SPI**

Effect of RH on the equilibrium water uptake values of SFm20, SAM20, and SAc20 sheets is shown in Figure 8. The equilibrium water uptakes of SFm20, SAM20, and SAc20 sheets decrease with a decrease of RH from 98% to 35%. Obviously, increasing the RH and plasticizer contents led to relatively high water uptake of the plastic sheets. Comparing to SAM20 and SAc20, the equilibrium water uptake of SFm20 is much lower, which resulted from the compact structure in SFm20. Therefore, formamide-plasticized soy protein materials exhibited higher water resistance than SAM and SAc.

Typical DSC thermogram curves of the SAM20 sheet under different RH are shown in Figure 9 and

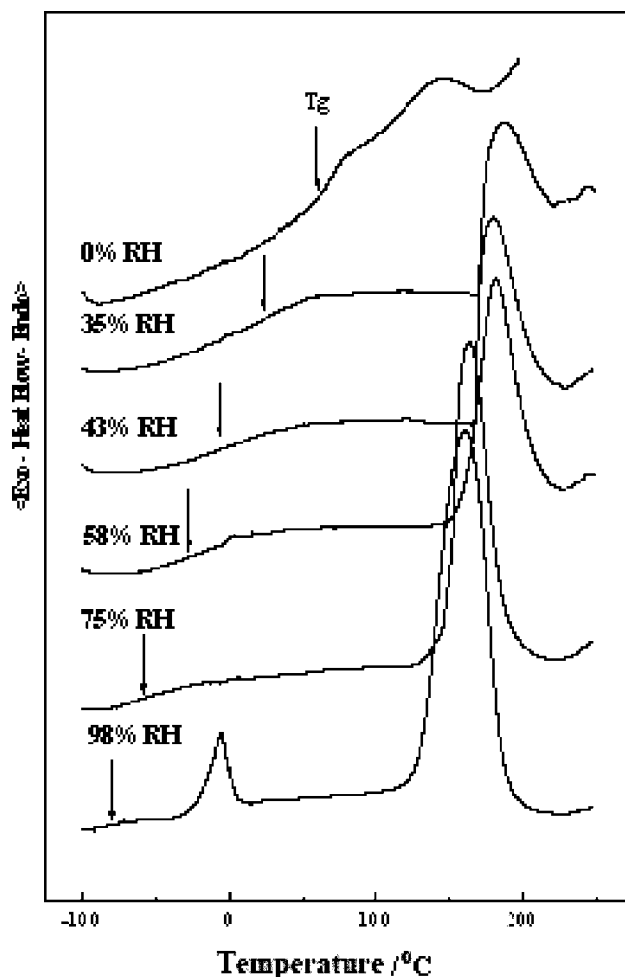
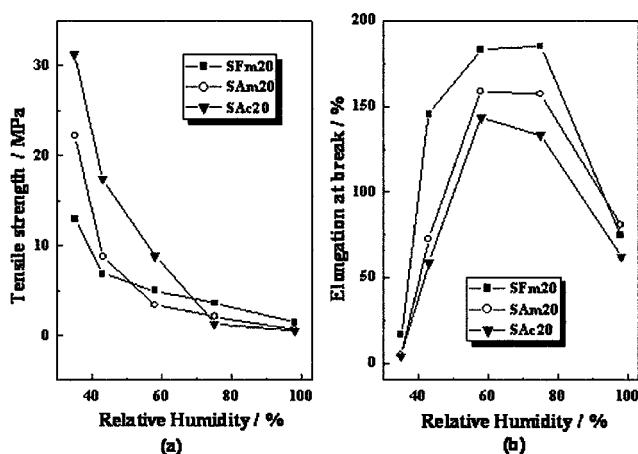


Figure 9 DSC thermograms of SAM20 sheets under different RH.



**Figure 10** Tensile strength (a) and elongation at break (b) of the SFm20, SAm20, and SAc20 sheets under different RH levels.

the resulting  $T_g$ s of SAm20, SFm20, and SAc20 are listed in Table I. Single  $T_g$  exhibits in every SAm20 sheet with different water uptake and it shifts to lower temperature with the increase of RH because the adsorbed water acted as a plasticizer. The endothermic peak at about 100°C indicated the amount of water in the SAm20 sheet. Its peak areas increased, whereas the temperature at peak position decreased with the increase of RH. A small endothermic peak at about 0°C, existing in DSC curve of SAm20 at 98% RH, was a crystal-melt peak of water. It is the fact that at high moisture a lot of free water lied in the interior or surface of sheets except much bound water. In high moisture condition  $T_g$ s of SFm20, SAm20, and SAc20 sheets are below 0°C as shown in Table I. This indicates that  $T_g$  values of the amide plasticized SPI plastics are dependent on moisture content to some extent.

Amides and water all play a role of plasticizer in natural polymer system,<sup>34,35</sup> such as soy protein plastics. Mechanical properties of the plasticized SPI sheets have been analyzed at ambient temperature as a function of nature of the plasticizer and moisture content. Tensile strength ( $\sigma_b$ ) and elongation at break ( $\epsilon_b$ ) of plasticized SPI sheets at different RH levels are shown in Figure 10. At low RH level (less than 58% RH), the  $\sigma_b$  value of SFm20 is lowest, whereas its elongation at break is highest of SFm20, SAm20, and SAc20 plastics. The increasing trends of brittleness shift from SFm20, SAm20, to SAc20 representing high  $\sigma_b$  but low  $\epsilon_b$  of the SAc20 sheets, which is in good agreement with the fact that  $T_g$  of SAc20 is higher than others. At high RH level (more than 58% RH),  $\sigma_b$  and  $\epsilon_b$  values of the sheets sharply decreases with the increase of moisture contents. Although at high RH levels  $\sigma_b$  and  $\epsilon_b$  values of SFm20 are higher than that of SAm20 and SAc20 on account of better water resistance, actually  $\sigma_b$  and  $\epsilon_b$

values of SFm20, SAm20, and SAc20 are relatively low. Therefore, it can be concluded that at low moisture content, amide plasticizers is the major factor that influence mechanical properties of soy protein plastics. However, at high moisture content, absorbed water as a plasticizer dominantly take into action. Always, the moisture content at about 60% is considered as "safe moisture content" for pure soy protein.<sup>36,37</sup> For amide plasticized soy protein materials 58% RH can be regarded as a "safe relative humidity". Therefore, amide plasticized soy protein materials only controlled under 58% RH should be utilized as plastics possessing good mechanical performances.

## CONCLUSIONS

Formamide and acrylamide were successfully used as plasticizers for soy protein besides acetamide. Relatively good plasticization effect was achieved when SPI were plasticized by formamide, acetamide, and acrylamide with 20, 30, and 30 phr, respectively. Single  $T_g$  of the SFm, SAm, and SAc sheets indicated homogenous structure and good compatibility. Comparing to acetamide and acrylamide, formamide was a high efficient plasticizer as a result of its smaller molecular weight, less steric hindrance, stronger hydrogen-bonding interaction with soy protein. The optical transmittance, flowability, and flexibility were significantly improved by adding amide as a plasticizer. Mechanical properties of soy protein plastics were also highly influenced by moisture content. At low RH, the mechanical property was mainly influenced by the nature and content of amides, whereas at high RH the tensile strength decreased sharply with increasing relative humidity as a result of the plasticization of water. Thus, it was suggested that it was safe to use these protein materials just under relative humidity of 58%.

## References

1. Paetau, I.; Chen, C. Z.; Jane, J. L. *Ind Eng Chem Res* 1994, 33, 1821.
2. Paetau, I.; Chen, C. Z.; Jane, J. L. *J Environ Polym Degrad* 1994, 2, 211.
3. Wang, S.; Zhang, S.; Jane, J. L.; Sue, H. *J Polym Mater Sci Eng (Am Chem Soc)* 1995, 72, 88.
4. Wang, S.; Sue, H.; Jane, J. L. *J Macromol Sci Pure Appl Chem (Ed) A* 1996, 33, 557.
5. Zhang, J. W.; Jiang, L.; Zhu, L.; Jane, J. L.; Mungara, P. *Biomacromolecules* 2006, 7, 1551.
6. Kawamura, Y.; Matsumura, Y.; Matoba, T.; Yonezawa, D.; Kito, M. *Cereal Chem* 1985, 62, 279.
7. Liu, Y.; Li, K. *Macromol Rapid Commun* 2002, 23, 739.
8. Liu, Y.; Li, K. *Macromol Rapid Commun* 2004, 25, 1835.
9. Shih, F. F. *J Am Oil Chem Soc* 1994, 71, 1281.
10. Stuchell, Y. M.; Krochta, J. M. *J Food Sci* 1994, 59, 1332.
11. Huang, X.; Netravali, A. N. *Biomacromolecules* 2006, 7, 2783.

12. Kumar, R.; Choudhary, V.; Mishra, S.; Varma, I. K.; Mattiason, B. *Ind Crop Prod* 2002, 16, 155.
13. Wool, R. P. *Chemtech* 1999, 29, 44.
14. Liu, K. *Soybeans—Chemistry, Technology, and Utilization*; International Thomson Publishing: New York, 1997.
15. Rahman, M.; Brazel, C. S. *Prog Polym Sci* 2004, 29, 1223.
16. Chen, P.; Zhang, L.; Cao, F. *Macromol Biosci* 2005, 5, 237.
17. Chen, P.; Zhang, L. *Macromol Biosci* 2005, 5, 872.
18. Chen, P.; Zhang, L. *Biomacromolecules* 2006, 7, 1700.
19. Ganeshsrinivas, E. Sathyanarayana, D. N.; Machida, K.; Miwa, Y. *J Mol Struct (Theochem)* 1996, 316, 217.
20. Liu, D.; Zhang, L. *Macromol Mater Eng* 2006, 291, 820.
21. Wu, Q.; Zhang, L. *J Appl Polym Sci* 2001, 82, 3373.
22. Vergnaud, J. M. *Liquid Transport Process in Polymeric Materials: Modeling and Industrial Application*; Prentice-Hall: Englewood Cliffs, NJ, 1991.
23. Anglès, M. N.; Dufresne, A. *Biomacromolecules* 2002, 3, 1101.
24. Anglès, M. N.; Dufresne, A. *Macromolecules* 2000, 33, 8344.
25. Lodha, P.; Netravali, A. N. *Ind Crop Prod* 2005, 21, 49.
26. Krause, S. *J Macromol Sci Rev: Macromol Chem* 1972, 7, 251.
27. Cooper, A. *Biophys Chem* 2000, 85, 25.
28. Redl, A.; Morel, M. H.; Bonicel, J.; Guilbert, S.; Vergnes, B. *Rheol Acta* 1999, 38, 311.
29. Pommet, M.; Redl, A.; Morel, M. H.; Guilbert, S. *Polymer* 2003, 44, 115.
30. Towns, J. K. *J Chromatogr A* 1995, 705, 115.
31. Brunauer, S.; Emmett, P. H.; Teller, E. *J Am Chem Soc* 1938, 60, 309.
32. Brunauer, S.; Deming, L. S.; Deming, W. E.; Teller, E. *J Am Chem Soc* 1940, 62, 1723.
33. Brooker, D. B.; Bakker-Arkema, F. W.; Hall, C. W. *Grain Equilibrium Moisture Content: Drying and Storage of Grains and Oilseeds*; Avi Publishing Company: New York, 1992.
34. Irissin-Mangata, J.; Bauduin, G.; Boutevin, B.; Gontard, N. *Eur Polym J* 2001, 37, 1533.
35. Audic, J. L.; Chaufer, B. *Eur Polym J* 2005, 41, 1934.
36. Hermansson, A. M. *J Food Protect* 1977, 12, 177.
37. Hermansson, A. M. *J Texture Stud* 1978, 9, 33.